Received: 21 July 2021 | Revised: 06 September 2021 | Accepted: 13 September 2021
DOI: 10.22034/ecc.2021.300767.1225
Eurasian Chemical Communications
SAMI

FULL PAPER

Removing methylene blue dye from industrial wastewater using polyacrylonitrile/iron oxide nanocomposite

Yasser Yousef Muhi-Alden* |**Khulood A. Saleh**

Department of Chemistry, College of Science, University of Baghdad, Baghdad, Iraq

***Corresponding Author:**
Yasser Yousef Muhi-Alden
Email:YasserYousif.Muhie1205@sc.uobaghdad.edu.iq
Tel.: + 009647706298699

Organic contaminants are present in industrial wastewater treatment procedures, and heavy metal ion removal is difficult. Photo Fenton reaction activity was exploited in this study to decompose organic contaminants using a functional composite hydrogel. The_hydrogel is made up of Fe_3O_4 particles, and Polyacrylonitrile (PAN). It was prepared by mixing in different proportions. And it has exceptional mechanical strength and Photo-Fenton activity as a result of various breakdown data that were influenced differently under pH, H_2O_2 concentration, dye concentration, temperature, and irradiation duration. Atomic Force Microscopy (AFM) was used to examine the composite's shape and average diameter. Under UV irradiation, the degradation(deg) of Methylene Blue dye (M.B) by the PAN/Fe_3O_4 hydrogel composite reached 99.7% after 60 min. This research proposes a new method for processing high-consistency industrial effluent that is difficult to decompose.

KEYWORDS

Photo-fenton reaction; PAN/Fe_3O_4 nanocomposite; methylene blue.

Introduction

Fenton is a cutting-edge therapeutic method. The hydroxyl radical (OH) is produced when aqueous ferrous ions combine with hydrogen peroxide (H_2O_2), and it has the ability to degrade refractory and hazardous organic in wastewater [1]. Fenton oxidation is an appealing and practical method for degrading huge volumes of hazardous organic pollutants. Fenton/oxidation technology can be divided into homogeneous and heterogeneous (Fenton-like) reactions. The homogeneous Fenton process also has apparent disadvantages, such as tight pH requirements, significant doses of catalyst agents (Fe^{2+}), and the generation of a considerable volume of ferric sludge that must be disposed [2]. This increases the number of reagents used. Solid, iron-containing compounds or solid materials are rich in iron, such as Fe_3O_4 [3,4]. As a result, addressing the Fenton process' drawbacks amounts to a never-ending research project in the field of refractory wastewater treatment using the Fenton technique. The heterogeneous Fenton process, fluidized-bed Fenton method, and electro-Fenton are only a few of the approaches used to overcome such constraints [5]. Hydrogels have recently gained popularity among 3D materials due to their ability to minimize photocatalyst aggregation, having high adsorption performance, providing convenient mass

transfer routes, and being easy to separate from the reaction solution. Furthermore, most hydrogels are physically robust and thermally stable, making them appealing in applications such as water purification, oil–water separation, and biomimetic materials. As a sustainable resource [6], composite gels are thought to improve the mechanical properties of hydrogels; for example, composite gels with a unique organic inorganic network structure have extraordinary mechanical properties [7]. In this sense, more complex polymeric systems, such as molecularly imprinted polymers, have evolved, allowing the procedure to be more selective [8]. The chemistry of PAN is of particular importance since it is used as a matrix in the development of carbon nanofiller-based nanocomposite for different appliances. Carbon nanotubes (CNT), graphene, and graphene oxide (GO) have all been employed in bulk composite materials and thin films [9]. Recently, there has been a surge of interest in the use of composite NFs in water treatment, especially for the removal of organic pollutants [10,11]. Chen et al., for example, found that calixarene-functionalized polyacrylonitrile (PAN) composite nanofibers NFs effectively adsorb Congo red [10]. To our understanding, however, the elimination of antibiotics by electrospun NFs has yet to be extensively investigated. Fe_3O_4/PAN composite 1D nanostructured Fe_3O_4 NPs and electrospun PAN NFs, which have high adsorption potential and are easy to separate from aqueous medium, are combined in composite NFs. Due to its low cost, ease of electrospinning, and high tensile strength after electrospinning, PAN was chosen as the prototype for Fe_3O_4 NPs deposition [12].

Experimental part

Determination of maximum absorption (λ max)

The wavelength value of M.B absorption is 650 nm used to estimate its quantity as shown in Figure 1.

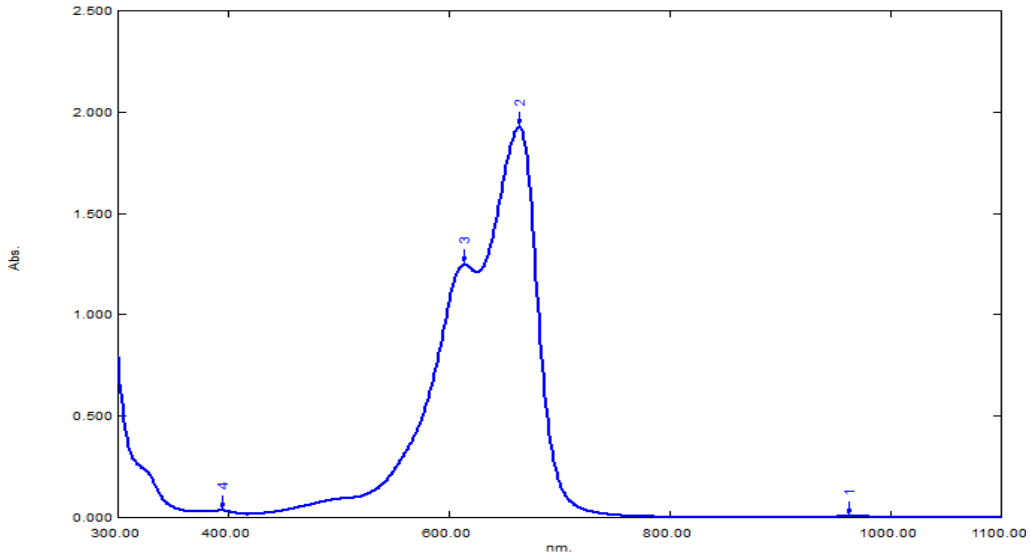

FIGURE 1 UV-Visible absorption spectrum for methylene blue dye

Calibration curve for M.B dye

Figure 2 illustrates the calibration curve which is the linear relationship between absorbance and concentration.

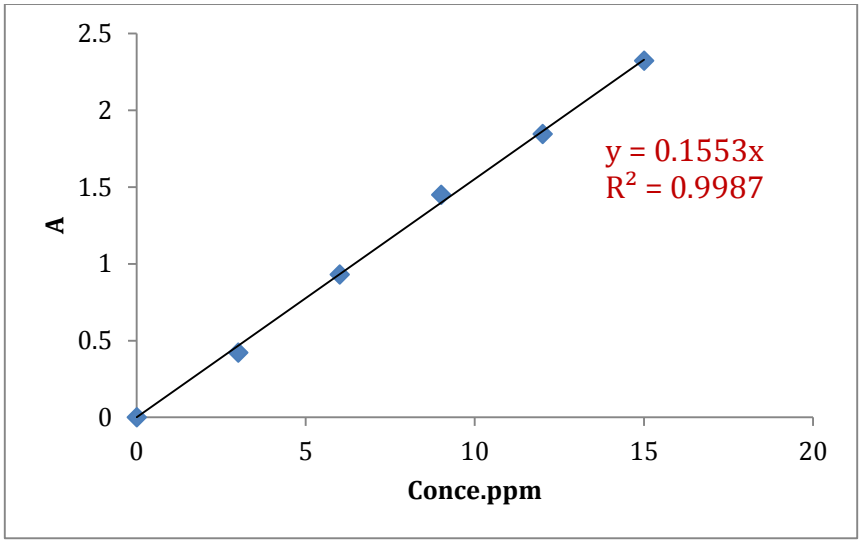

FIGURE 2 Calibration curve for methylene blue

Polyacrylonitrile/iron oxide nanocomposite preparation

To create excellent and consistent nanofibers, the combination of PAN and nanoparticle has been adjusted. The Fe_3O_4 combination of PAN and nanoparticle has been tweaked to produce good and consistent nanofibers. The Fe_3O_4 nanoparticles were added into distilled water and subjected to ultrasonic agitation overnight to prevent aggregation. Following that, PAN was added to the dispersed Fe_3O_4 nanoparticles by stirring and heating (60 °C) after dispersion (Fe_3O_4 nanoparticles - 20 nm in diameter).

Preparation of photocell

Stainless-steel pipe with 1 cm diameter and 15 cm length Figure 3 was supplied with a copper coil surrounded by the external cell by drop surface and with water bath attached to them. The temperature of the reactor and the lamp solution should be kept under control. The inner cellular surface was first treated with strong HF acid to make it rough and capable of capturing the casing, and then the cell was entirely coated with PAN/Fe_3O_4 nanocomposite for 10 minutes to allow the production of a stable layer, and then the suspension was released from the reactor. To make the catalytic layer more stable as a coating, the photo reactor displays 500oC in the inner reactor surface.

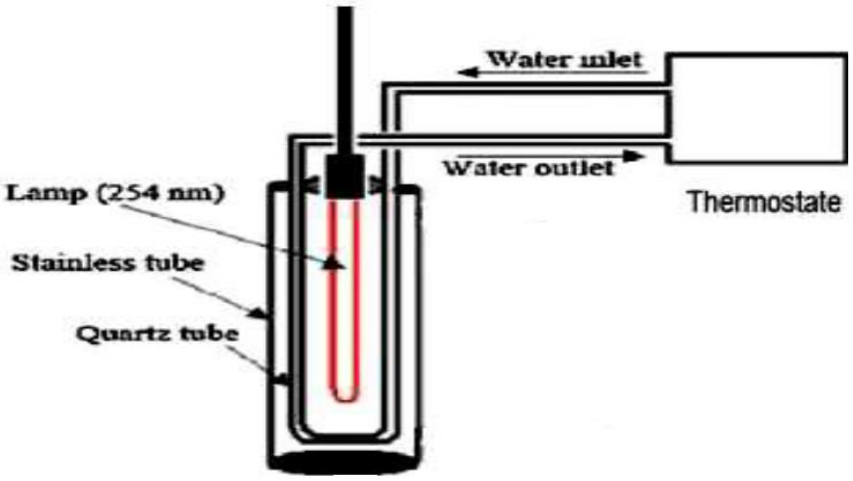

FIGURE 3 Complete system set up for photo degradation

Kinetic degradation study

The following first order equation No. (1) was applied in the study of kinetic decomposition

$$\text{Ln Ce} = \text{Ln C0} - \text{Kt} \quad (1)$$

Where: Co: initial concentration of M.B (ppm). C**t**: Concentration of M.B (ppm) after exposing to UV at time t.

The following Arrhenius equation No. (2) was applied to calculated kinetic parameter Ea**,A** [13]:

$$\text{Ln k} = \text{Ln A} - \text{Ea/R} \quad (2)$$

Where T: is the absolute temperature (in kelvins), k is the rate constant, Ea is the reaction's activation energy (in k.J mol^{-1}), A is the pre-exponential factor, and R is the global gas constant.

Results and discussion

Atomic force microscope (AFM)

The AFM analysis provides the measurements of average grain size and the granularity cumulating distribution for PAN/Fe_3O_4 nanocomposite. The average diameter is 89.17 nm PAN / Fe_3O_4 nanocomposite. Figure 4 shows the atomic microscopy image for PAN/ Fe_3O_4 nanocomposite.

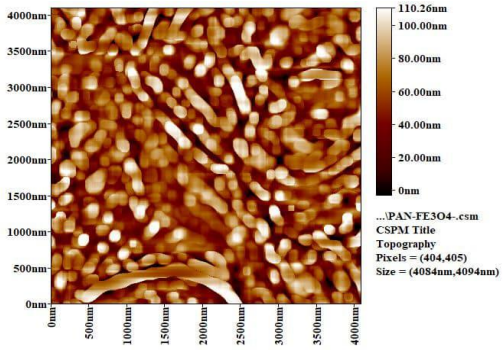

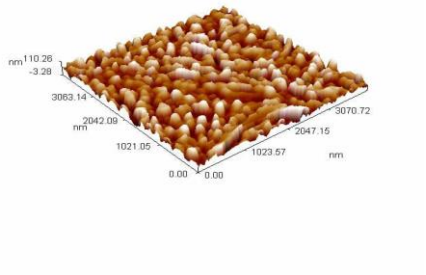

FIGURE 4 Atomic microscopy image of PAN/Fe_3O_4

Effect of Fe_3O_4 concentration

The effect of Fe_3O_4 concentration on %deg of M.B dye using PAN on M.B %deg was investigated for three different weights (0.05, 0.1, 0.5) g at the following conditions: pH=7, H_2O_2 concentration 5*10-3 M and 298K; the results in Figure 5 show that the best %deg of M.B. was by using 0.1 g Fe_3O_4 .

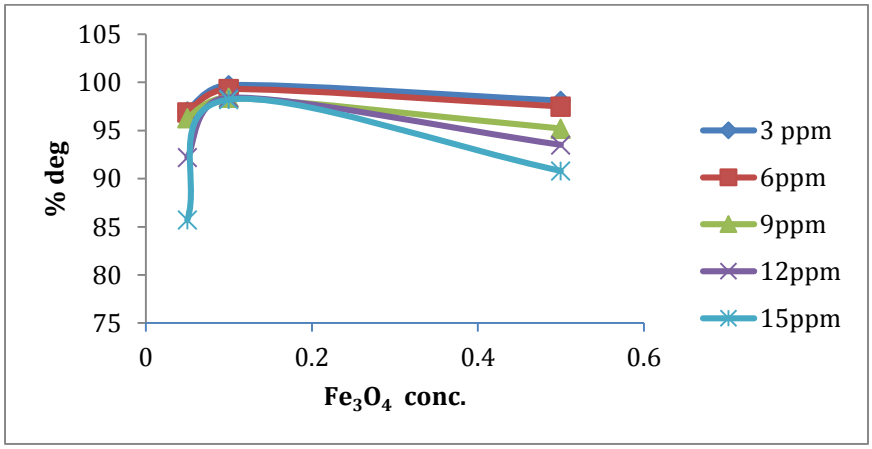

FIGURE 5 Effect of Fe_3O_4 concentration variation for different M.B concentration on %deg. after 60 min, at temp. 298K, pH=7 and H_2O_2= 5*10-3 M

Effect of initial concentration

To study the effect of initial concentration of dye on the degradation efficiency, the experiments used included different initial concentration (3-21) ppm at pH=7, temperature 298K and 5*10⁻3 M H_2O_2 catalyst PAN/ Fe_3O_4 nanocomposite after 60 min. as shown in Figure 6. The increase of degradation percentage in each time happened with the decrease of M.B concentration, reaching the highest value 99.7% for 3 ppm M.B dye concentration. This phenomenon can be explained according to the indication that the number of the dye molecules will be increased with constant number regarding •OH. Also, with the increase in dye's initial concentrations, extra molecules have been adsorbed onto catalyst's surface [14], leading to decreasing in oxidation process.

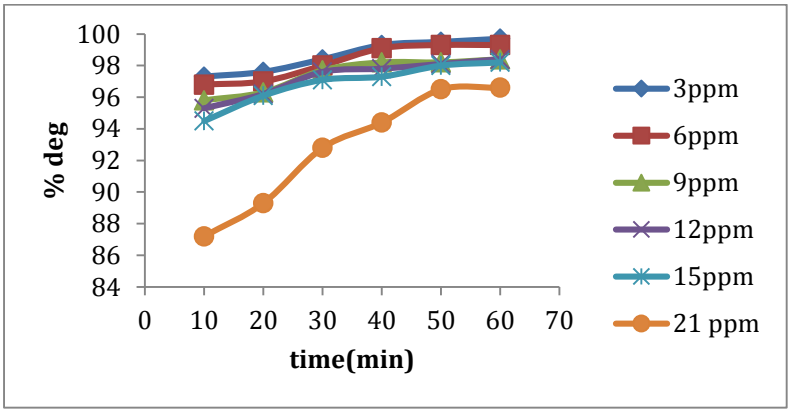

FIGURE 6 Variation of (%deg) with time for different M.B concentration at 298K, pH=7 and H_2O_2 5*10-3 M by PAN/Fe_3O_4 catalyst

Effect of H_2O_2 Concentration

The effect of H_2O_2 concentration on the M.B dye degradation was studied at temperature 289K, pH=7, and after 30 min in presence of catalyst PAN/Fe_3O_4 nanocomposite, the decolorization percentage (%deg.) increased with a rise in H_2O_2 concentration, which is shown in Figure 7. 3 ppm of M.B dye degradation is (96.8) % in case the concentration of H_2O_2 is (3*10-3M) after 30 min. The degradation percentage reaches (94.2) % in case of using (1.6*10-3M) H_2O_2 after 30 min. For high M.B dye concentration (15 ppm), low H_2O_2 concentration (0.8*10-3M) leads to degradation percentage reaching (87.5)%. With increasing H_2O_2 concentration from (0.8* 10-3M) to (5*10-3M), the decolorization percentage increases, which can be specified via the impact regarding the additionally created OH• radicals. Yet, with additional H_2O_2 concentrations, reaction rate levels off and is often badly impacted, through gradual increase of hydrogen peroxide. This happens because of auto decomposition of H_2O_2 to oxygen and water in addition to the re-combination regarding the OH• radicals (reactions 1 and 2) [15].

$2H_2O_2 \rightarrow H_2O + O2$ .... (1)

$OH• + 2H_2O_2 \rightarrow OH• 2 + H2O$ ..... (2)

The excess that is related to H_2O_2 is going to react with the OH• competing with organic pollutants and thus decreasing the treatment's effectiveness; H_2O_2 will contribute to OH• radicals scavenging capacity. Nevertheless, a higher dose of H_2O_2 means a higher production of hydroxyl radicals and this dose increases because the higher H_2O_2 concentration is more favored for the occurrence of auto scavenging reactions. Therefore, H_2O_2 should be added at an optimal concentration to achieve the best degradation, but above these, range improvement was not obvious.

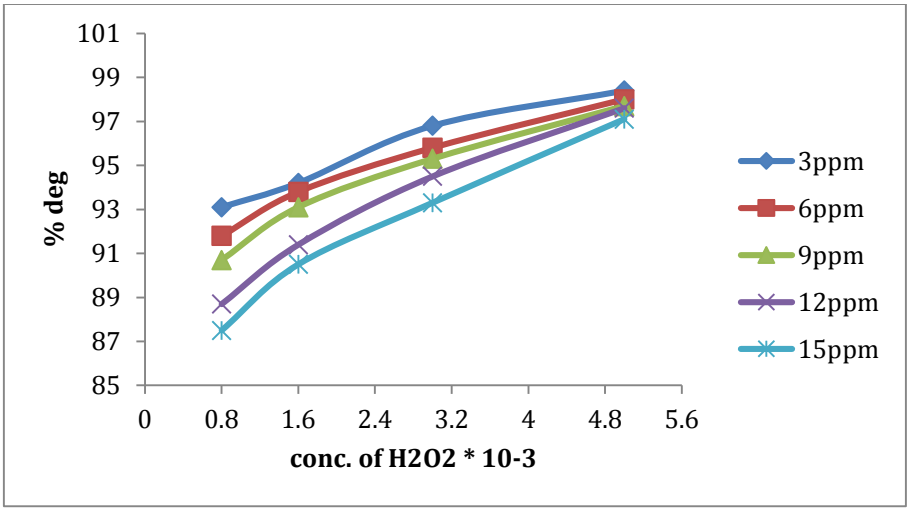

FIGURE 7 Effect of varying H_2O_2 concentration for different M.B concentration after 30 min, at 298K, pH=7 on PAN/ Fe_3O_4 nanocomposite catalyst

Effect of temperature

The influence of temperature on (3 ppm) M.B percent deg by PAN/Fe_3O_4 nanocomposite at four different temperature (298, 308, 318, and 328) K at pH=7 was examined. As seen in Figure 8, the results showed that, the % deg. of 3 ppm on PAN/ Fe_3O_4 nanocomposite increases from 99.7% in temperature 298K to 100% at 318K and the % deg. of 15 ppm on PAN/Fe_3O_4 nanocomposite increases by increasing temperature from 98.7% at 298K to 99.2% at 318K that indicates obeying Arrhenius relation [15]. At a temperature of (328), the dissolution of the dye decreases at different concentrations that indicated an anti- Arrhenius relation. The disappearance of M.B during the first 60 min of oxidation could be described as first-order reaction kinetics with regard to M.B concentration.

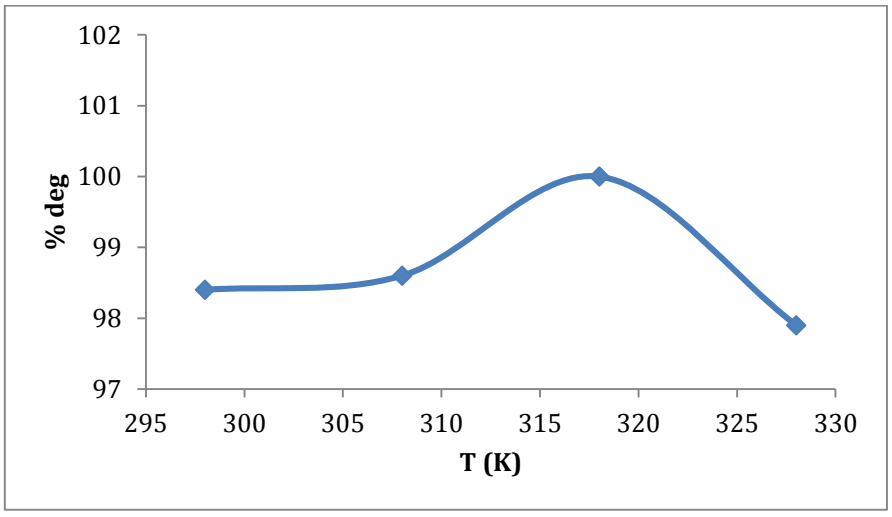

FIGURE 8 Variation of 3 ppm M.B %deg by PAN/ Fe_3O_4 nanocomposite with different temperature

Kinetic degradation study by PAN/Fe_3O_4 nanocomposite catalysts

Using a PAN/Fe_3O_4 nanocomposite, Equation No. (1) of the first order was applied to the decomposition process of 12 ppm MB at a H_2O_2 concentration of 0.005 M: time and space after UV exposure at the specified time. Figure 9 shows the linear relationships between LnCe and the time for degradation of the 12 ppm MB dye at four temperatures.

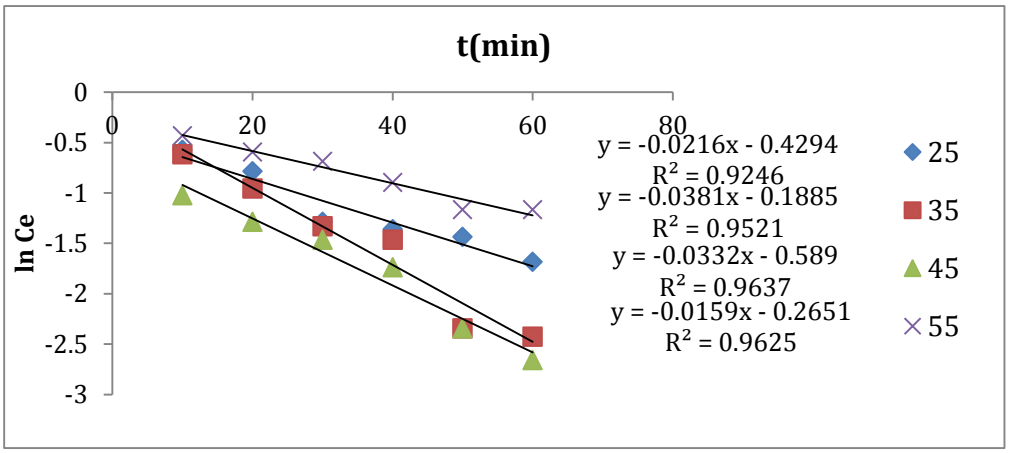

FIGURE 9 LnCe V.S time for the degradation of 12 ppm M.B at four temperatures by using three catalysts: PAN/Fe_3O_4 nanocomposite

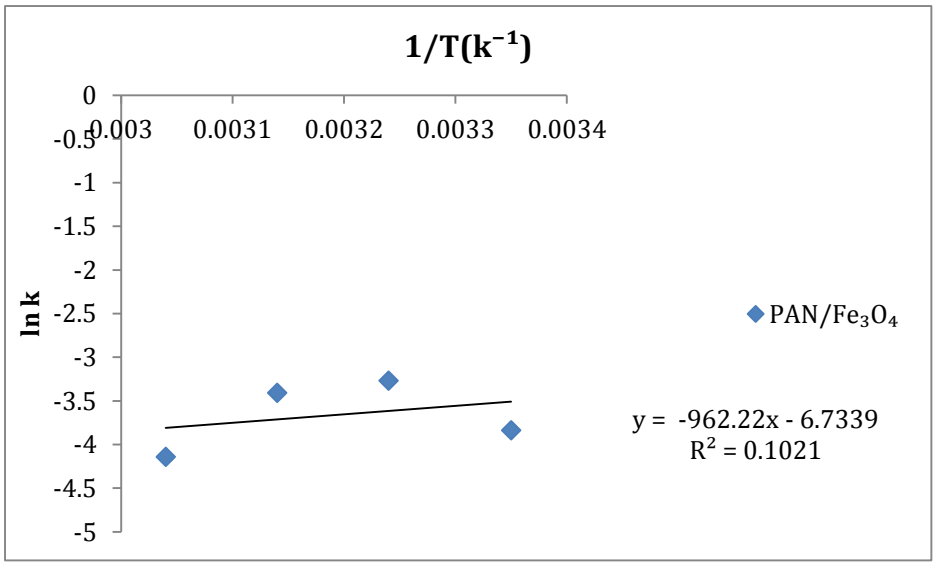

FIGURE 10 Arrhenius plots, relation Lnk with 1/T for the12 ppm M.B %deg. PAN/Fe_3O nanocomposite

Arrhenius equation No. (2) has been applied to calculate the kinetic parameter A, Ea. The activation energy, also known as the minimum energy necessary to initiate a chemical reaction, of degradation is represented by Ea, while the pre-exponential factor in the rate equation is represented by A Figure 10. Table 1 below shows the values of Ea and A obtained from the slope and intercept of the Ln k versus 1/T plot.

TABLE 1 Kinetic parameter for PAN//Fe_3O_4 nanocomposite

	T(K)	k/(min)10-3	Ln k	Ea/KJ.mol^{-1}	A (min^{-1})
PAN//Fe_3O_4	298	21.6	-3.835	7.9	0.0001
	308	38.1	-3.267		
	318	33.2	-3.405		
	328	15.9	-4.141		

Conclusion

In conclusion, we investigated the Methylene Blue dye degradation capacity in PAN/Fe_3O_4 nanocomposite as a catalyst, which was prepared in laboratory. AFM was used to characterize the composite, including its average diameter and shape. The particle size increases after adding Fe_3O_4 nanocomposite to PAN, and the percent degradation efficiency for M.B increases, according to AFM image

analysis. Using a PAN/Fe_3O_4 nanocomposite as a catalyst, the Photo-Fenton method was effectively used to remove the contaminants dye. The optimum irradiation time was determined to be 60 minutes. The pH impact revealed that Ph=7 had the best degradation of M.B dye on PAN/Fe_3O_4 nanocomposite. The degradation of M.B dyes on the PAN/Fe_3O_4 nanocomposite increased with increasing temperature but decreased at temperature (328k), according to the temperature impact data. After the dye solution has been subjected to irradiation for a longer amount of time, the color has been totally eliminated and the dye has been transformed into organic material. M.B dye degradation on PAN/Fe_3O_4 nanocomposite was well interpreted with the first order, according to the kinetic research findings. Finally, the utilized approach (photo Fenton procedure) is suggested for the treatment of organic compound-containing wastewater.

Acknowledgements

I would like to express my deepest gratitude to all staff members of Department of Chemistry, College of Science, University of Baghdad for their support and encouragement.

References

[1] M. Xu, C. Wu, Y. Zhou, *Adv. Oxid. Process.*, **2020**, 61. [crossref], [Google Scholar], [Publisher]

[2] J. Du, B. Zhang, J. Li, B. Lai, *Chinese Chem. Lett.*, **2020**, *31*, 2575–2582. [crossref], [Google Scholar], [Publisher]

[3] B. Iurascu, I. Siminiceanu, D. Vione, M. A. Vicente, A. Gil, *Water Res.*, **2009**, *43*, 1313–1322. [crossref], [Google Scholar], [Publisher]

[4]L. Xu, J. Wang, *Appl. Catal. B Environ.*, **2012**, *123*, 117–126. [crossref], [Google Scholar], [Publisher]

[5] D. Ghernaout, N. Elboughdiri, S. Ghareba, *Open Access Libr. J.*, **2020**, *7*, ID: 979641. [crossref], [Google Scholar], [Publisher]

[6] Z. Du, F. Liu, C. Xiao, Y. Dan, L. Jiang, *J. Mater. Sci.*, **2021**, *56*, 913–926. [crossref], [Google Scholar], [Publisher]

[7] W.L. Hom, S.R. Bhatia, *Polymer*, **2017**, *109*, 170–175. [crossref], [Google Scholar], [Publisher]

[8] B.F. Urbano, S. Bustamante, D.A. Palacio, M. Vera, B.L. Rivas, *Polym. Int.*, **2020**, *69*, 333–345. [crossref], [Google Scholar], [Publisher]

[9] A. Kausar, S. Anwar, *Polym. Plast. Technol. Eng.*, **2018**, *57*, 565–580. [crossref], [Google Scholar], [Publisher]

[10] M. Chen, C. Wang, W. Fang, J. Wang, W. Zhang, G. Jin, G. Diao, *Langmuir*, **2013**, *29*, 11858–11867. [crossref], [Google Scholar], [Publisher]

[11] M. Teng, J. Qiao, F. Li, P.K. Bera, *Carbon*, **2012**, *50*, 2877–2886. [crossref], [Google Scholar], [Publisher]

[12] D. Zhang, A.B. Karki, D. Rutman, D.P. Young, A. Wang, D. Cocke, T.H. Ho, Z. Guo, *Polymer*, **2009**, *50*, 4189–4198. [crossref], [Google Scholar], [Publisher]

[13] S. Arrhenius, *Zeitschrift für Phys. Chemie*, **1889**, *4U*, 96–116. [crossref], [Google Scholar], [Publisher]

[14] R.A. Faris, Z.F. Mahdi, M.D. Abd. Husein, *IOP Conf. Ser.: Mater. Sci. Eng.*, **2020**, *871*, 012019. [crossref], [Google Scholar], [Publisher]

[15] A.M.T. Allayla, R.A. Faris, Z.F. Mahdi, *Vib. Spectrosc.*, **2021**, *114*, 103252, [crossref], [Google Scholar], [Publisher]

How to cite this article: Yasser Yousef Muhi-Alden*, Khulood A. Saleh. Removing methylene blue dye from industrial wastewater using polyacrylonitrile/iron oxide nanocomposite. *Eurasian Chemical Communications*, 2021, 3(10), 755-762. **Link:** http://www.echemcom.com/article_136946.html